

A spatially-explicit study of prey-predator interactions in larval fish: assessing the influence of food and predator abundance on growth and survival

P. **Pepin**¹, J. F. **Dower**², F.J.M. Davidson³

Abstract

We apply a coupled bio-physical model of transport to reconstruct the environmental history of larval radiated shanny in Conception Bay, Newfoundland. The model is applied to data collected during a two week period during which larvae, their food (**copepod** nauplii) and their predators (capelin) were monitored in three intensive surveys. Our goal is to determine whether environmentally explicit information can be used to infer the characteristics of individual larvae which are 'most likely to survive. Backward reconstruction is used to assess the influence of variations in the feeding environment on changes in the growth rates of individual larvae. Forward projections are used to assess the impact of predators on the cumulative density distribution of growth rates on the population of larvae in different areas of the bay. An individual's past growth has a strong influence on the pattern of growth during the course of our study. There was relatively little influence of current feeding conditions on increment widths for larvae less than 15 days old but there was some evidence of a slight positive influence of increasing prey abundance on growth beyond this age, although this was not statistically significant. Patterns of selective mortality suggest that fast growing individuals suffered higher mortality rates, suggesting they are growing into a predator's prey field. However, the mortality rates appeared to increase with decreasing predator abundance, based on the drift reconstructions. The relationship of growth and mortality with environmental conditions suggests that short-term, small scale variations in environmental history may be difficult to describe accurately in this relatively small system (1000 km²).

¹ Department of Fisheries and Oceans, P. O. Box 5667, St. John's, NF Canada **A1C 5X1**
Tel: 1-709-772-208 1; Fax: -4 105; E-mail: **pepin@athena.nwafc.nf.ca**

² Department of Earth and Oceans Sciences, University of British Columbia, Vancouver, B.C. Canada **V6T 124**

³ Department of Physics and Physical Oceanography, Memorial University of Newfoundland, St. John's, NF Canada **A1C 5S7**

INTRODUCTION

Which individual fish larvae survive **from** hatch to metamorphosis (or during some other ecological or physiological shift) will depend not only on each individual's growth rate but also on the spatial and temporal pattern in the selective forces which they encounter. Regional differences in feeding and growth may alter the relative susceptibility to impact by predators (**Rilling** and Houde 1999) and the variable movement of highly active and migratory species, such as pelagic fish, may result in differential survival patterns. For example, Paradis et al. (1999) found that variations in the timing of simulated predation pressure resulted in substantial difference in the distribution of growth rates found in surviving fish larvae.

How we investigate the effect of environmental conditions on either individual growth histories or on their distribution within the population is critical. To determine how an individual responds to changes in its feeding environment requires that we be able to reconstruct the pattern of **drift** of that individual, at least in a general sense. Once we have captured the larva, we must be able to provide a backward projection of drift. Furthermore, we must consider that the growth of an individual at some age x is highly dependent on the growth rate during previous days (**Mosegaard** et al. 1988; **Pepin** et al. submitted). The response to changes in prey availability may not be immediate. If on the other hand we are concerned with the selective removal of individuals from the population (e.g. by predators), then we cannot focus on individual growth rates but rather on the distribution of growth rates within the population. We must then project the pattern of drift forward for different parcels of the population to assess the changes in the distribution of growth histories, or any other measure of condition (**Pepin** et al. 1999), in relation to the environmental conditions which they encounter. We cannot simply infer the processes that have affected larvae based on the conditions they are associated with when we sample them: we have to be able to infer where they came from (or go to) and what conditions they encountered along the way.

Patch studies have been used to track the movement of larval fish but they provide a detailed view of only a small portion of the population and can generally be carried out for only short periods (Davis et al. 1991; Murdoch and Quigley 1994; **Pepin** et al. submitted). An alternative is to couple survey observations with a dynamic circulation model that provides a reliable forecast of the variations in current speed and direction over the study area (**Bowen** et al. 1995; Taggart et al. 1996). The patterns of transport and dispersal can then be used to develop the history of individuals caught at each sampling site either by forward or backward projections. The approach will be limited by the accuracy of the circulation model and the temporal horizon of the projections.

We apply the concepts we discussed above to study the patterns of growth and survival of radiated shanny larvae (*Ulvaria subbifurcata*). Our observations are based on three surveys of Conception Bay (47°45'N, 53 °00'W) during which we sampled the ichthyoplankton and their prey using plankton nets and in addition, monitored the abundance of capelin (*Mallotus villosus*), the dominant planktivorous pelagic fish in the area, using hydroacoustic integration. Growth histories were derived from measurements of otolith microstructure and the **drift** was simulated

using a fine-resolution wind-driven 3-D eddy resolving circulation model.

MATERIALS AND METHODS

Field Sampling

The specimens used in this analysis were collected as part of a population study of the larval fish community in Conception Bay, Canada (**47°45'N, 53 °00'W**). Details of the study site were described previously (**Laprise and Pepin 1995**). Three surveys, separated by one week, were conducted between 20 July and 5 August, 1998. Ichthyoplankton were sampled at 19-23 stations spaced approximately 8 km apart and located throughout the bay (Fig. 1). Each survey was conducted in approximately 24 hours. At each station, a single oblique tow (0-40 m) was performed using a 4 m² Tucker trawl equipped with sections of 1000, 570, and 333 µm mesh nitex (**Pepin and Shears 1997**) and towed for 10- 15 minutes at 1 m s⁻¹. Volume filtered during the tow was estimated as the average of two General **Oceanics** flow-meters located at mouth of the net. Samples were preserved in 95% ethanol. After one week, samples were drained to replace the preservative. Ichthyoplankton were subsequently sorted and identified to species or to the lowest taxonomic level possible. The length frequency distribution for each species and sample was estimated by measuring up to 200 larvae. Standard length was measured to the nearest millimeter using a dissecting microscope and a gridded background.

Microzooplankton were sampled using a 0.5 m diameter plankton net (70 µm mesh) hauled vertically from 40 m to the surface (1 m s⁻¹). Samples were preserved in 2% buffered formaldehyde. The abundance of **copepod** nauplii was estimated by sequential fractionation of the sample using a Metoda splitter until approximately 200 individuals could be identified and enumerated.

Temperature, salinity and fluorescence profiles of the water column were obtained at each station using a **Seabird-25** CTD (sampling rate of 8 Hz) lowered at a rate of 1 m s⁻¹ to within 5 m of the bottom.

Currents were measured using a hull-mounted Acoustic Doppler Current Profiler (ADCP: **153kHz**) to provide a basis for comparison with the circulation model. Data **from** the ADCP, operated in bottom track mode, were recorded in 4 m depth bins (first bin at 7-11 m). A sampling interval of 2 minutes was used to give a nominal ensemble average based on at least 50 pings. The standard deviation of unsmoothed single bin currents was ~ 0.03-0.05 m s⁻¹.

An **EK500** echosounder (**38kHz**) was used to measure the abundance of pelagic fish by hydroacoustic integration. Data from the **EK500** were recorded for depth bins of 5-20, 20-35, 35-50, 50-75, 75-100 and 100-200 m using 3 minute integration intervals with a threshold of -65 dB.

Otolith microstructure analysis

Body measurements of larval shanny were taken using an Optimas **image analysis system (V.4.1)** connected to a dissecting microscope. An Olympus BH-2 compound microscope (**500x magnification**) and imaging system were used for all otolith measurements. Prior to otolith extraction, each animal was given a unique identifier number and measured for standard and **total** length to the nearest 0.1 mm. Lapillar and sagittal otoliths were extracted from 509 specimens of *U. subbifurcata* (up to 10 larvae were selected at random from each station). Each otolith was mounted in a small drop of Crystal Bond® thermoplastic cement placed on a microscope slide. All subsequent analyses were performed using the **sagitta**, choosing the right or **left** otolith at random unless one proved impossible to read. Each otolith was ground to the mid-plane using 0.3 μm lapping film. Minimum and maximum radius as well as the hatch check were measured relative to the nucleus of the otolith. Total area was estimated by identifying the periphery of the otolith. The operator then measured the width of each increment by marking the outer edge of that increment along the longest axis of each otolith, which occasionally required refocusing of the image. A second independent measurement of increment widths was performed by the same reader on 203 of the 509 previously analysed otoliths. The assessment of measurement error is presented elsewhere (**Pepin et al. submitted**). Throughout the analysis, we consider that each otolith increment represents one day. Analyses of patterns in increment widths were performed using data standardized to zero mean and unit standard deviation ($z_{i,j} = (x_{i,j} - \bar{x}_j) / s_j$, for specimen i in age interval j) because of the changes in mean increment width **with increasing age** (**Pepin et al. submitted**).

To assess the potential impact of selective mortality on larval shanny, we had to contrast the distribution of growth histories from one survey to the next among larvae of the same age during the initial survey. To achieve this, age-dependent cumulative probability distributions (CDF) were derived using local non-parametric density estimation (Davison and Hinkley 1997; **Pepin et al. 1999**). The CDF of increment widths **from** the one survey was then contrasted with the CDF for larvae caught in subsequent survey at the ages they had during the earlier survey (e.g. contrast width in 10 day old larvae caught in the first survey with the widths found at age 10 in 17 day old fish caught in the second survey). Because of the level of autocorrelation in increment widths (**Pepin et al. submitted**), the data **from** each individual included widths the three increments preceding the day of capture (for the initial conditions) or the back-calculated age during the initial survey (for the larvae captured in surveys 2 or 3). We only include the three increments in order to avoid biasing our estimates of the CDF with growth histories for which we have no environmental information. The significance of changes in the age-dependent pattern of median increment width was determined by calculating the 95% confidence intervals of the median using randomization.

Drift Simulations

Simulations of the circulation during the study period were performed with the 3-D eddy resolving CANDLE model of Davidson et al. (2000). This z-coordinate model solves the 3-D

non-linear Navier-Stokes equations on an f-plane using the hydrostatic, Boussinesq and rigid-lid approximations. The equations are finite **difference**d on a 3-D, Arakawa C-grid with 1 km horizontal and 10 m vertical resolution. A free-slip condition is applied on the lateral land boundaries. The model domain comprised of a realistic bottom topography of Conception Bay, and of Trinity Bay to the north, whose wind driven circulation has an influence on Conception Bay by means of coastal trapped wave propagation.. The open boundary conditions are similar to those of Greatbatch and **Otterson** (1991). These are a no normal gradient boundary condition applied to horizontal velocity components and density. In addition, the northern model's open boundary is an extension of the coastline at Cape Bonavista, preventing the occurrence of spurious upwelling at the juncture of land and open boundary (Greatbatch and Otterson, 1991), which could then propagate into the model domain.

All circulation model runs are initialized at rest (i.e. no motion) with horizontally uniform stratification based on the long term mean (1957-1997) for the month of July at Station 27 (approx. 20 km south of the mouth of Conception Bay). The model is run with spatially uniform wind stress based on observations at St. John's Airport, situated 10 km west of Conception Bay. Wind stress is introduced over 2 days using a hyperbolic tangent ramping function starting on day 190 and running for 35 days. Particles are released on day 201 at 12 am. The drifter mode implemented is described in Davidson and **deYoung** (1995) and is designed to track particles smoothly through a finite resolution velocity field. There is no vertical transport of drifters so particles are constrained to a 2-D velocity field within each layer. Particles will thus accumulate near the coast where downwelling occurs. The drifters were given a random walk component to their displacement at every time step equivalent to a **diffusion** coefficient of $10 \text{ m}^2 \text{ s}^{-1}$. This allows for particles seeded at the same location in the model to be dispersed from each other over time.

Backward projections of larval drift tracks were conducted by uniformly seeding the model domain with particles (0.5 km apart) on days 201 and 208 and simulating their **drift** for 7 days. At the end of the simulation period, particles were assigned to a station location, sampled on days 208 and 215, only if they are located within 3 km of the sampling site. Forward projections were performed by seeding 1000 particles within a 1 km radius of the stations sampled on days 201 and 208 and forecasting their **drift** for a 7 day period. A 14 day simulation was also performed starting with the station locations sampled on day 201. We analyzed the patterns of **drift** for the top two **modelled** layers (0-10 and 10-20 m) to correspond to the observed vertical distribution of larvae in the upper water column. As the results were similar for both layers despite differences in responsiveness to wind forcing, we only present the results from the second for the sake of brevity.

Because we cannot assign the behaviour of an individual particle to an individual larva caught at a sampling location, we calculated the average drift trajectory of the particles assigned to each station for both the backward or forward projections. This introduces a level of uncertainty in the source or destination of particles as we move away (backward or forward in time) from the survey when larvae were sampled. In both instances, dispersion will move particles away from the centre of mass leading to increased uncertainty about the environmental conditions which the

larvae are likely to have encountered.

Environmental reconstructions were based on the observations collected during each of the three surveys. For each realization, data **from** stations (for **copepod** nauplii) or continuous collections (for pelagic fish) were interpolated onto a 1 km grid. Because we did not have sufficient information to describe the movement, and production in the case of nauplii, the changes in environmental conditions **from** one survey to the next were linearly interpolated through time at each grid point. The conditions encountered by the larvae **from** each station (either in backward or forward projections) were then determined using the positional information from the average **drift** trajectory at daily intervals **from** the start to the end of each simulation period. When the average drift trajectory wandered outside the area within which we could interpolate environmental conditions, we did not attempt to extrapolate conditions to the station's position. Environmental reconstructions were performed for each 7 day period.

Forward **drift** projections were used to investigate patterns of mortality. The concentration of larvae **from** each station sampled on days 201 or 208 was moved to the model's projected location and contrasted with the abundance of larvae observed on days 208 and 215 respectively. To account for the effects of growth, the abundance of larvae of length l (each interval being of 1 mm) on day t was contrasted with the abundance of larvae of length $l+2$ observed on day $t+7$ and mortality rates were calculated as $Z = \ln(N_{l+2, t+7}/N_{l, t})$. Our choice of a 2 mm increment is based on observed growth rates (see below).

RESULTS

Environmental Conditions

There were no major shifts in wind forcing during the study period. Winds were predominantly **from** the southwest at average speeds of $\sim 20 \text{ km h}^{-1}$ with speeds rarely exceeding 30 km h^{-1} (Fig.2). There were two instances where the wind **shifted** to westerly/northerly direction but average speeds decreased to $\sim 10 \text{ km h}^{-1}$. These bouts lasted 28 and 36 hours and were generally preceded by periods with weak southwesterly winds. There was also a short period of weak westerly toward the end of the study period.

Surface temperature exhibited similar spatial patterns during all surveys with warmer waters on the eastern side and cooler ones in the western region (Fig.3). There was an eastward movement of the surface isotherms between the first and second surveys followed by a retraction toward the western side of the bay between the second and third sampling periods (Fig.3). Changes between the second and third surveys also increased the contrast in surface temperatures between western and eastern regions, possibly indicating an increase in upwelling. Over the course of the study, average density stratification among all survey sites increases in the top 40 m of the water column due to a combination of upwelling and surface heating. This increased mean vertical density gradient is associated with a significant increase in fluorescence (Fig.4).

The overall abundance of nauplii was lowest during the first survey and highest during the second, with a decrease **from** those levels during the third sampling period (Fig.5). The changes in overall abundance may reflect variations in secondary production in response to increases in phytoplankton abundance. Variations in the spatial distribution of **copepod** nauplii from one survey to the next mimicked the **shifts** in the distribution of surface temperature (Fig.3). There was a significant expansion of a region of high nauplii concentration during the second survey followed by a gradual retraction of the area toward the western side of the bay.

Hydroacoustic returns indicated a steady decrease in the abundance of pelagic fish during the course of the study (Fig.5). Overall average acoustic returns decreased three-fold between the first and third surveys. Because the hydroacoustic data were collected continuously rather than at a restricted number of stations, we can observe greater detail in the spatial distribution than was possible for **copepod** nauplii. During the first survey, acoustic targets were broadly distributed throughout the study area with the highest concentrations found seaward of Bell Island (Fig. 5). The distribution of pelagic fish showed a greater degree of patchiness during the second sampling period, with the highest concentrations located on the western side but with the greater levels still being found in the outer portion of the bay (Fig.5). Low concentrations were present throughout the bay during the third survey with small areas of high concentrations scattered in the outer part of the bay (Fig.5).

Currents measured during the surveys provide only a snapshot of the circulation pattern during various portions of the survey. Although estimates of the currents are not corrected for tidal flows, we know that these are only of the order of $\sim 2 \text{ cm s}^{-1}$ and thus do not represent a major contribution to the pattern of observations. Vertically averaged currents measured using the ADCP between 7 and 27 m show considerable horizontal spatial variability. There was evidence of counter-clockwise recirculation in the outer portion of the bay during the first and third surveys with an area of divergence along the northeastern shore apparent during all three surveys. During the first survey, flow in the southern part of the bay was in a southerly direction on the eastern side and northwesterly on the western side. Currents measured during the second survey are directed into the bay along the western side and generally flow toward the mouth along the eastern shore. There was no discernable pattern observed during the third survey, other than a tendency for weak westerly or northerly currents along the western side. Currents became progressively weaker during the study period with an average of 8.7 cm s^{-1} (range: 1-29), 7.7 cm s^{-1} (range: 1-19) and 4.9 cm s^{-1} (range: 1-12) **from** the first to the third survey.

Drift Projections

The general circulation pattern observed throughout the study period was characterized by a clockwise flow with a relatively strong north-eastward current along the western side (Fig.6). Currents, and thus drift, were stronger during the first part of the study (days 201-208) than during the second (days 208-215). There was greater evidence of a retentive gyre in the outer portion of the bay during the latter period. Average drift trajectories suggest that movement of particles along the eastern side of the bay appears to have been somewhat less important during

both surveys but this is largely an artefact of the location of sampling sites that are used to initialize the simulations (Fig.6). The trajectory of individual particles clearly shows the existence of a clockwise gyre with significant drift along the eastern side of the bay (Fig.6). Backward and forward projections indicate that the head of the bay is a major source of particles for the outer portion of the bay (**Fig.7**). A two week projection of **drift** shows that most of the larvae which were at the head of the bay (based on 6 stations) at the **start** of the study (day 201) would have drifted into the outer portions of the study area by day 215 (Fig.7).

Changes in the distribution of larvae between surveys supports the projections based on the circulation model. During the first survey, many of the larvae were located at the mouth of the bay (**Fig.8**). Based on a 2 mm increment in length between surveys (see below), major larval concentration moved along the south into the inner bay and **further** along onto the western shore. From the second to the third survey, major concentrations of larvae had progressed further north along the western portion of the bay (Fig.8).

Despite spatial differences in the distribution of prey and predators, the reconstructions of environmental histories were dominated by the major shifts in abundance that took place from one survey to the next (Fig.9). The shift in mean nauplii concentration based on the backward projections from one survey to the next was substantially greater (- 10: 1) than the variability among stations within a survey (Table 1). Forward projections of predator conditions showed that the shift in mean predator levels between surveys was slightly less than the variance among stations within surveys (**Fig.9**), but in contrast to the pattern exhibited for nauplii, both statistics were approximately of the same order.

The average growth rate of radiated **shanny** larvae, based on length at age of capture, was 0.29 mm d^{-1} ($F_{111[1,504]} = 2830, P < 0.001$) and there were no statistically significant differences among surveys ($F_{111[2,504]} = 0.91, P > 0.5$) (Fig. 10).

Analysis of growth histories in relation to the reconstructed feeding environment from the backward **drift** projections showed that the average increment width at the start of each observation period (days 201 or 208) was the single most important variable determining the growth of individual larvae during the study period. Exploratory analysis revealed that there was a significant interaction between the age at which the increment width was measured and the average individual increment width for the three days prior to the start of each **drift** reconstruction. Consequently, we analyzed the pattern of growth increment widths for each age class (post hatch) separately. The model we applied described the increment width on day of life (i.e. age) i (g_i) in relation to the average increment width on the three days prior to day 201 or 208 (G), the forward lag from that day (Δt), and the concentration of nauplii encountered on day i (N_i) based on the backward drift simulations ($g_i = b_0 + b_1 G + b_2 \Delta t + b_3 N_i$ where the b_j s refer to regression coefficients). The older the larvae were, the stronger and more direct the effect of their past history on their current growth (Fig. 11). There was a negative effect of the forward separation from the start of each simulation period, which was significant for most ages between 10 and 25 days (Fig. 11). This effect is mostly an artefact of the standardization of increment

widths coupled with the pattern of selective survival in relation to past growth. Finally, there was little evidence of a significant effect of nauplii abundance on the growth of individual larvae (Fig. 11). Only for ages of 10 and 12 days posthatch was the effect significant, and in those instances the relationships was negative. The trend was for the regression coefficients to be negative for ages 5-13 and mostly positive for ages 14-26. A runs test shows this pattern to be significant ($P < 0.05$) but the effect is so weak relative to other factors that the biological significance appears to be nearly inconsequential.

The overall pattern of changes in abundance clearly indicates that mortality rates **increase** with increasing length of larvae (Fig. 12). Losses were greater during the **second** week of the study relative to the first. In some instances there appears to have been an increase in abundance rather than a decrease, particularly in the smaller larvae during the first period of observation (Fig. 12). This is partly because our approach to estimate the “mortality history” does not allow for dispersal or aggregation of larvae in the model domain but rather uses the average **drift** path to determine the centre of mass of particles from each source station. The relationship between mortality rates and the history of predator encounters is in the opposite direction to expectations: mortality rates decrease with increases in the estimated predator field (Fig. 12). A multivariate general linear model revealed a strong significant effect of body length on mortality ($F_{[11,139]} = 78.8, P < 0.001$) and a significant interaction of body length with predator density ($F_{[11,139]} = 13.7, P < 0.05$). Restricting the analyses to 1 mm length intervals revealed that decreases in mortality rate with increasing predator density were only significant in the largest size category (13 mm) but notable in all length intervals **from** 10 mm onward (Fig. 13). In smaller length categories the response to changes in reconstructed predator abundance was essentially flat. Finally, we estimated the degree of overlap between larvae and their predators during the first and second surveys using Williamson et al’s (1989) index ($O = m \sum N n / [\sum N \sum n]$ where N and n represent the abundance of larvae and predators estimated **from** the interpolated fields) for each 1 mm larval length category. Overlap between larvae and pelagic fish was substantially higher for the length categories **from** 10-12 mm during the second survey (Fig. 14) suggesting that the higher mortality rates during the second week could have been due to higher overall interactions between prey and predation.

Because of the strong contrast in predator abundance between the inner and outer portions of the bay, we use the separation between stations above and below the northern tip of Bell Island to contrast the distribution of increment widths (based on the last three increments before capture) from one survey to the next. Larvae caught during the first survey in the inner bay showed an increasing median standardized increment width with increasing age in contrast to larvae in the outer bay which showed a slight decrease (Fig. 15). The contrast in trends with age between regions is not quite as pronounced during the second survey but it is still present and increment widths in the inner bay are generally higher than in the outer bay (Fig. 15). There is almost no difference in the pattern of growth histories between the inner and outer bay during the final survey (Fig. 15).

To provide an appropriate contrast of the changes in the CDF of growth increments through time,

we must take into consideration the results of the drift projection which show substantial movement of larvae from the first survey **from** the inner to the outer **portions of the bay (Fig.6)**. This results in almost complete transport of particles **from** the inner bay into the distal **part of the** system by the end of the second week (Fig.7). In contrast, larvae **from** the outer **bay** tend to remain in that region although there is some transport into the inner part of the study site. If we consider the inner bay exclusively, there is selective removal of faster growing larvae **from** the first through to the third survey (Fig. 16). The median increment width is significantly lower during survey 2 for larvae that were ages 19 and beyond in survey 1 and for ages 9 and beyond when we contrast surveys 1 and 3. When we compare larvae **from** the inner (survey 1) and outer bays (surveys 2 and **3**), which may be a more appropriate comparison based on our **drift** projections, the median increment width is significant lower in larvae that would have been older than 10 and 4 days old during the first survey (Fig. 16). Comparing larvae in the outer bay reveals a significant decrease in increment widths **after** two weeks (surveys 1 and 3) in larvae that were less than 15 days of age during the first survey but there is no significant difference in older larvae (Fig. 16). When we contrast larvae from the second and third surveys, we find significant differences in the median only between the inner and outer portions of the bay (Fig. 17). In virtually all instances, there is evidence of selective removal of faster growing larvae during our study.

DISCUSSION

Growth histories of individuals and their distribution within the population have provided us with an indication about some of the processes acting on the dynamics of radiated shanny larvae. An individual's history was found to have a profound effect on the growth observed between each survey period but we were unable to find any compelling evidence that the environmental history significantly altered the growth of an individual. At the population level, there was clear evidence of selective mortality in which faster growing individuals were less likely to survive than individuals with lower growth rates. This is consistent with the pattern of increasing mortality with increasing body size. However, we were again unable to find a relationship to perceived environmental history (in this case predator abundance) consistent with fundamental expectations. One is **left** to question whether our projections of circulation were accurate and whether there was any benefit in developing environmental histories?

Conception Bay is a physically dynamic system which responds rapidly to variations in wind forcing as a result of both local and remote influences (**deYoung** et al. 1993). Davidson et al. (2000) showed their model was able to predict changes in both surface circulation as well as in the rise and fall of isopycnals. Prior to and during the study period winds were light and generally from a constant direction. Under southwesterly wind conditions, the dominant currents along the western side of the bay flow along the coast and generate upwelling. Model projections indicated stronger currents during the first week of our study and weaker ones during the second. Our observations of surface temperatures are consistent with these predictions as cold waters were more widely distributed during the second survey than in the first but their extent receded by the end of the second week. Furthermore, the shifts in the distribution of larvae with time were also

consistent with the presence of a clockwise circulation field with an area of retention or convergence located in the northwestern quadrant of the system. These patterns suggest that the general features of the circulation were adequately represented by the model's forecast for the purposes of this study.

Environmental histories are essential if we are to understand the **dynamics** of larval fish. We know from an analysis of measurement error of otolith microstructure that contemporary observations of environmental conditions are unlikely to yield much insight into the **processes** regulating growth because the width of growth increments just before capture reflect the effects of past rather than present events (**Pepin** et al. submitted). However, without knowledge of the **drift** and the environment which the larvae encountered we would not have been able to assess the possible influence of prey availability on increment widths. Spatial and temporal scales of the system under study and the variations in the environmental conditions must also be considered in assessing the understanding gained in this study. The general correspondence of changes in prey distributions with changes in the extent of cold water, and to a lesser extent the temporal variations in abundance, suggests that the general magnitude of fluctuations were reasonably well captured by our sampling program. Fluctuations in nauplii abundance are likely to follow scales that are close to those of the physical environment. Our representation of the predator environment was probably inadequate. Although the high resolution of hydroacoustic data permitted a more detailed picture of the spatial distribution during the course of each survey, we have no information movement within the bay or about immigration or emigration. Migration patterns of pelagic fish can result in rapid changes in the abundance of these animals in small systems and their pattern of variation has considerable energy at small time and space scales (Home and Schneider 1994). In a larger study site, relative movement of predators would likely be less important, and a more accurate view of spatial and temporal variations in abundance could be achieved by repeated sampling. On scales such as those studied by Heath et al. (1998), the extent of spatial and temporal variations in environmental features may be more readily detected in the reconstruction of environmental histories. However, we were able to provide a gross characterization of the changes in predator abundance in the inner and outer parts of the bay that allow a better interpretation of the patterns in survival.

Individual growth histories play a significant role in determining future growth patterns and the importance of the past plays an increasing role as radiated shanny larvae age (**Pepin** et al. submitted; this study). We found a consistent pattern for a subtle positive and statistically non-significant influence of increasing prey abundance on growth in older larvae. Other studies have noted similarly small effects of the feeding environment on growth histories (**Gallego** et al. 1996). The appearance of an inverse relationship in larvae younger than 13 days post hatch is unexpected but measurement error is considerable in early increments (**Pepin** et al. submitted) so that any environmental influence may be more difficult to detect. The lack of a strong relationship with the prey environment suggests that events at the scale of the individual may be important in determining an individual's growth and survival potential. Processes at the individual level may be difficult to identify because of our inability to describe environmental variation at very small scales. The effect of small scale turbulence on radiated shanny larvae can only be characterized in

broad terms with substantial changes in environmental conditions (Dower et al. 1998). Factors such as parental influences may play an important role in determining an individual's growth potential (**Benoît** and **Pepin** 1999; **GrønkJær** and Schytte 1999; Hoeie et al. 1999) but these may be difficult to identify in a mixed population without knowledge of the state of the adult population. There is some indication that the level of variation in growth histories within individuals may provide some insight into the characteristics of potential survivors. The distribution of growth histories within and among larvae may yield some insight into the processes that lead **different** growth rates but this will require **further** study. What may also be required is to understand how external selection forces will determine which patterns of growth are more likely to survive.

Predation is one of the major factors influencing patterns of survival in larval fish but it is also one of the most poorly understood. Laboratory and enclosure studies have demonstrated that the vulnerability of fish larvae to predators is dependent on the size of both prey and predator (Bailey and Houde 1989; Fuiman and Marguran 1994; Paradis et al. 1996; Sogard 1998). Maximum vulnerability occurs when larval length is 10% of the predator's and it decreases on either side of this value (Paradis et al. 1996). In this study, we **focussed** on the role of pelagic fish because previous work had indicated that invertebrate carnivores, which are mostly small, were unlikely to significantly affect survival (Paradis and **Pepin** In press). Although we were unable to find a pattern of mortality in relation to predator abundance that was consistent with the expectation of a positive trend, both the increase in mortality with increasing length and the selective removal of fast growing larvae from the population suggests that pelagic fish are likely to be an important factor influencing losses **from** the population. Capelin sampled in Conception Bay in 1998 range from 8 to 18 cm in length (**Pepin** unpublished data) which implies that larval fish should be becoming more vulnerable to this predator as they grow. Until predation pressure is reduced (e.g. through emigration out of the area), low growth rates are likely to provide a short term survival advantage when considered over a fixed time interval (Paradis et al. 1999). However, before we can move beyond deducing the role of pelagic fish in determining patterns of **survival** in larval **from** corollaries we must better understand the patterns of encounter between prey and predator.

A few field studies dealing with the potential impact of invertebrate carnivores have found evidence that mortality rates are correlated with the abundance of these predators that can lead to spatial differences in population dynamics (**Taggart** and Leggett 1987; Pilling and Houde 1999). The influence of pelagic fish has been more difficult to **identify** although there is evidence of increased egg mortality with higher pelagic fish abundance (Smith et al. 1989). The association of mortality with invertebrate carnivore levels may be more easily detected because both prey and predator are similarly subject to transport which could maintain the overlap so that the impact can be identified. In a *post hoc* analysis, we were able to characterize two broad regions (inner and outer bay) with substantially different environmental histories in terms of predator abundance. Drift of larvae from the inner to the outer bay, **from** a region of apparent low predator abundance to one with higher levels, was associated with the disappearance of fast growing larvae from the population by the end of the second week. However, the short term changes that took place between surveys did not provide an adequate description of the encounters between predator and

prey. This is in contrast with a series of short term patch studies which show greater population losses in the presence of greater numbers of juvenile and adult capelin (**Pepin** and Dower unpublished data). Intensive surveys of local conditions enabled us to follow fluctuations environmental conditions more closely than could be done on a broader scale and thus we could identify substantial differences among systems that covered a large range in levels of predator abundance. How to move **from** small spatial and short time scales of observations to local or population levels requires better approaches to describing the movement of active predators.

ACKNOWLEDGEMENTS

We thank T. Shears for his efforts to coordinate the logistic and technical activities in both the field and in the laboratory. The assistance of H. Benoit, A. Bochdansky, S. Carter and K. Fleming in the field was invaluable and the careful analysis of otolith microstructure by C. **Mercer** is gratefully acknowledged. The work could not have been carried out with the assistance and expertise of the officers and crew of the *Wilfred Templeman*.

References

- Bailey, K.M. and Houde, E.D. 1989. Predation on eggs and larvae of marine fishes and the recruitment problem. *Adv. Mar. Biol.* 25: 1-83.
- Benoit, H.P. and **Pepin**, P. 1999. The interaction of rearing temperature and maternal influence on egg development rates and larval size at hatch in Yellowtail flounder (Pleuronectes ferrugineus). *Can. J. Fish. Aquat. Sci.* 56: 785-794.
- Bowen**, A.J., Griffin, D.A., **Hazen**, D.G., Matheson, S.A. and Thompson, K.R. 1995. Shipboard nowcasting of shelf circulation. *Cont. Shelf Res.* 15, 155-128.
- Davidson, F.J.M. and **deYoung**, B. 1995. Modeling advection of cod eggs and larvae on the Newfoundland Shelf *Fish. Oceanogr.* 4: 33-51.
- Davidson, F.J.M., Greatbatch, R.J. and **deYoung**, B. 2000. Asymmetry in the response of a stratified coastal embayment to wind forcing. *J. Geophys. Res.* In press.
- Davis, T.L.O., Lyne, V. and Jenkins, G.P. 1991. Advection, dispersion and mortality of a patch of southern bluefin tuna larvae Thunnus maccoyii in the East Indian Ocean. *Mar. Ecol. Prog. Ser.* 73: 33-45.
- deYoung**, B., Otterson, T. and Greatbatch, R.J. 1993. The local and nonlocal response of Conception Bay to wind forcing. *J. Phys. Oceanogr.* 23 : 2617-2635.
- Dower, J.F., **Pepin**, P. and Leggett, W.C. 1998. Enhanced gut fullness and an apparent shift in size-selectivity by radiated shanny (Ulvaria subbifurcata) larvae in response to increased turbulence. *Can. J. Fish. Aquat. Sci.* 55: 128-142.
- Fuiman**, L.A. and **Margurran**, A.E. 1994. Development of predator defences in fishes. *Rev. Fish Biol.* 4: 145-183.
- Greatbatch, R. J. and Otterson, T. 1991. On the formulation of open boundary conditions at the mouth of a bay. *J. Geophys. Res.* 96: 18431- 18445.

- Heath, M., Zenitani, H., Watanabe, Y., Kimura, R. and Ishida, M. 1998. Modelling the dispersal of larval Japanese sardine, Sardinops melanostictus, by the Kuroshio current in 1993 and 1994. *Fish. Oceanogr.* 7: 335-346.
- Hoeie, H., Folkvord, A. and Johannessen, A. 1999. Maternal, paternal and temperature effects on otolith size of young herring (Clupea harengus L.) larvae. *J. Exp. Mar. Biol. Ecol.* 234: 167-184.
- Home, J.K. and Schneider, D.C. 1994. Lack of spatial coherence of predators with prey: a bioenergetic explanation for Atlantic cod feeding on capelin. *J. Fish. Biol.* 45: 191-207.
- Gallego, A., Heath, M.R., McKenzie, E. and Cargill, L.H.. 1996. Environmentally induced short-term variability in the growth rates of larval herring. *Mar. Ecol. Prog. Ser.* 137: 11-23.
- Grønkjær, P. and Schytte, M. 1999. Non-random mortality of Baltic cod larvae inferred from otolith hatch-check sizes. *Mar. Ecol. Prog. Ser.* 181: 53-59.
- Laprise, R. and Pepin, P. 1995. Factors influencing the spatio-temporal occurrence of fish eggs and larvae in a northern physically-dynamic coastal environment. *Mar. Ecol. Prog. Ser.* 122: 73-92.
- Mosegaard, H., Svedang, H. and Taberman, K. 1988. Uncoupling of somatic and otolith growth rates in Arctic char (Salvelinus alpinus) as an effect of differences in temperature response. *Can. J. Fish. Aquat. Sci.* 45: 1514-1524.
- Murdoch, R.C. and Quigley, B. 1994. Patch study of mortality, growth and feeding of the southern gadoid Macruronus novaezelandiae. *Mar. Biol.* 121: 23-33.
- Paradis, A.R., Pepin, P. and Brown, J.A. 1996. Vulnerability to predation of fish eggs and larvae: a review of the influence of the relative size of prey and predator. *Can. J. Fish. Aquat. Sci.* 53: 1226-1235.
- Paradis, A.R., Pépin, M. and Pepin, P. 1999. An individual-based model of the size-selective vulnerability of fish larvae to four major predator types: disentangling the effect of size-dependent encounter rates and susceptibility to predation. *Can. J. Fish. Aquat. Sci.* 56: 1562-1575.
- Pepin, P., Dower, J.F. and Benoit, H.P. Submitted. Use of otolith increment width in the study of growth in larval fish: understanding the structure within.
- Pepin, P., Evans, G.T. and Shears, T.H. 1999. Patterns of RNA/DNA ratios in larval fish and their relationship to survival in the field. *ICES J. Mar. Sci.* 56: 697-706.
- Pepin, P. and Shears, T.H. 1997. Variability and capture efficiency of bongo and Tucker trawl samplers in the collection of ichthyoplankton and other macrozooplankton. *Can. J. Fish. Aquat. Sci.* 54: 765-773.
- Rilling, G.C. and Houde, E.D. 1999. Regional and temporal variability in growth and mortality of bay anchovy, Anchoa mitchilli, larvae in Chesapeake Bay. *Fish. Bull.* 97: 555-569.
- Smith, P.E., Santander, H. and Alheit, J. 1989. Comparison of the mortality rates of Pacific sardine, Sardinops sagax, and Peruvian anchovy, Engraulis ringens, eggs off Peru. *Fish. Bull.* 87: 497-508.
- Sogard, S.M. 1997. Size-selective mortality in the juvenile stage of teleost fishes: A review. *Bull. Mar. Sci.* 60: 1129-1157.
- Taggart, C.T. and Leggett, W.C. 1987. Short-term mortality in post emergent capelin Mallotus villosus. I. Analysis of multiple in situ estimates. *Mar. Ecol. Prog. Ser.* 41: 205-217.

- Taggart, C.T., Thompson, K.R., **Maillet**, G.L., **Lochman**, S.E. and Griffin, D.A., 1996. Abundance distribution of larval cod (**Gadus morhua**) and zooplankton in a gyre-like water mass on the **Scotian** Shelf. p. 155-173, In Y. Watanabe, Y. Yamashita and Y. **Oozeki** (ed.) Survival strategies in early life stages of marine resources. A.A. Balkema, Rotterdam.
- Williamson, C.E., Stoeckel, M.E. and Schoenecl, L.J. 1989. Predation risk and the structure of freshwater zooplankton communities. *Oecologia* **79**: 76-82.

Table 1. Change in environmental conditions (mean and variance in prey and predator abundance) among stations between successive surveys. All data were log-transformed.

		Day 201-208	Day 208-215
Nauplii	$\bar{x}_{\log(N)}$	3.80 – 4.24	4.31 – 3.98
	$s^2_{\log(N)}$	0.033 – 0.024	0.028 – 0.044
Predators	$\bar{x}_{\log(P)}$	-0.81 – -1.85	-1.16 – -2.55
	$s^2_{\log(P)}$	1.61 – 1.18	0.45 – 1.41

Figure 1 Map of survey area and station locations. Numbers next to station locations refer to locations used in drift projections in Figures 6 and 7. The solid line represents the separation between the inner and outer portions of the bay.

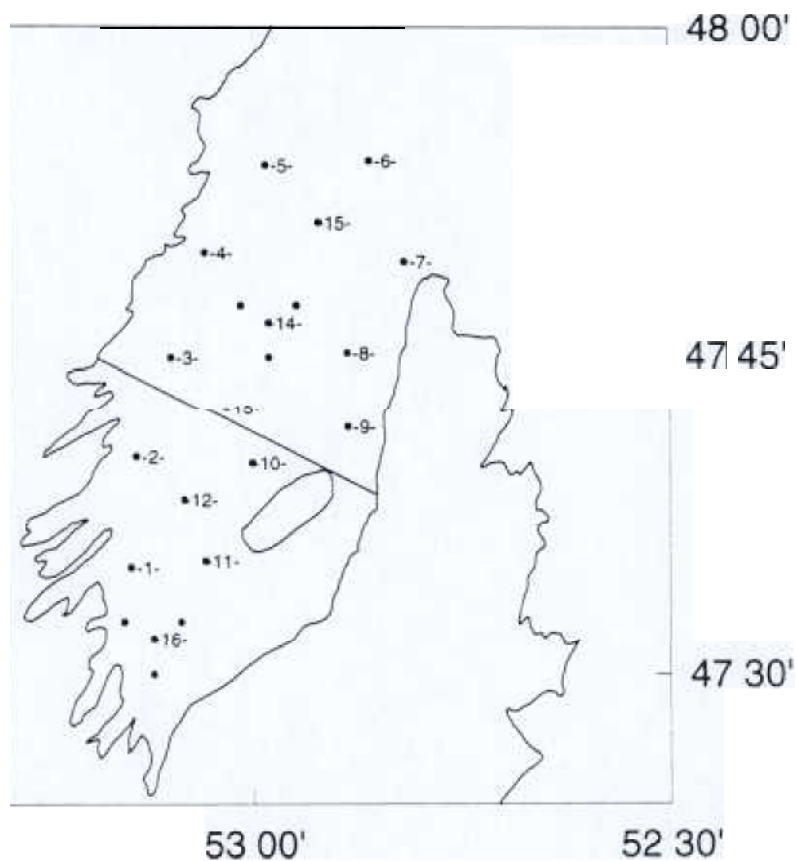


Figure 2.

Time series of wind speed (Top panel) and direction (Bottom panel) starting 5 days before the survey period (days 201-215) from the St. John's International Airport weather station. Data are recorded at hourly intervals.

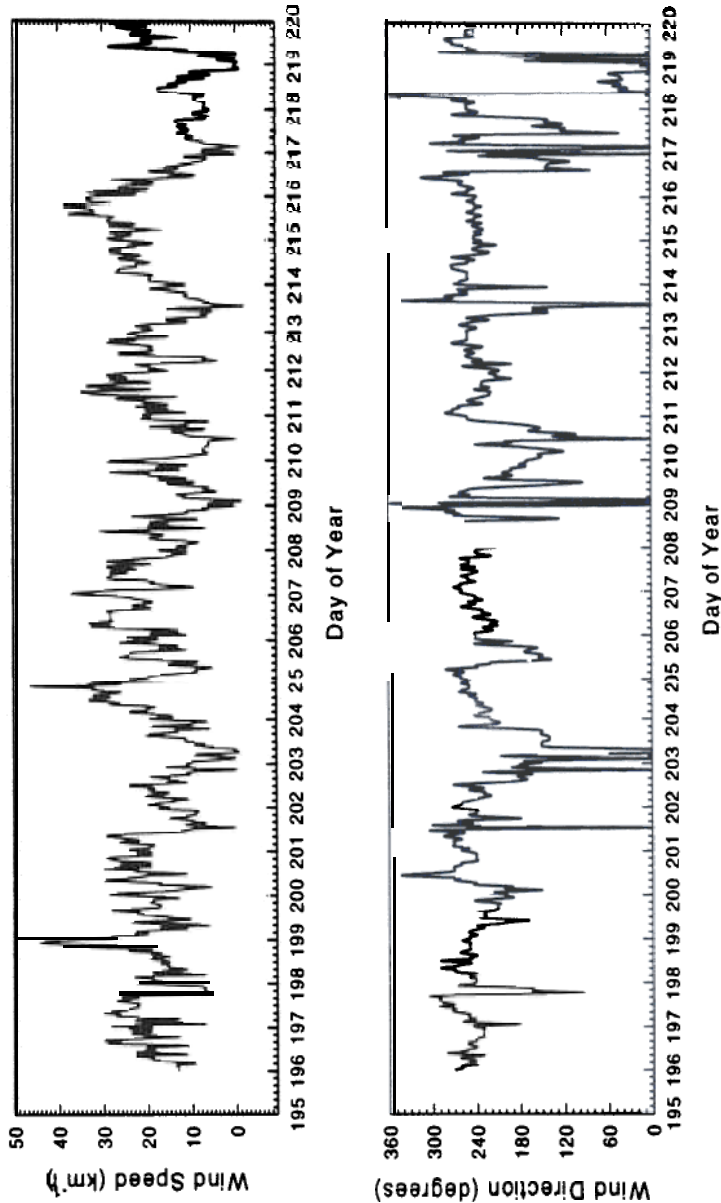
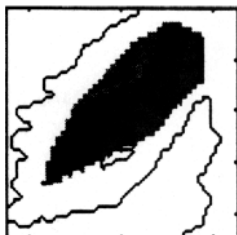
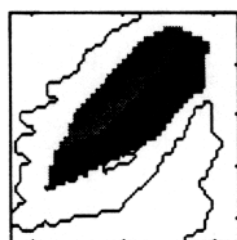


Figure 3. Sea surface (5 m) temperature (degrees Celsius) field during the three successive surveys of Conception Bay.

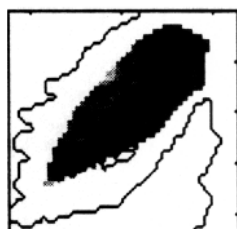
Temperature day 201



Temperature day 208



Temperature day 215



Average
sampled

per

(solid
Fj

density

and fluorescence

profile used the average all

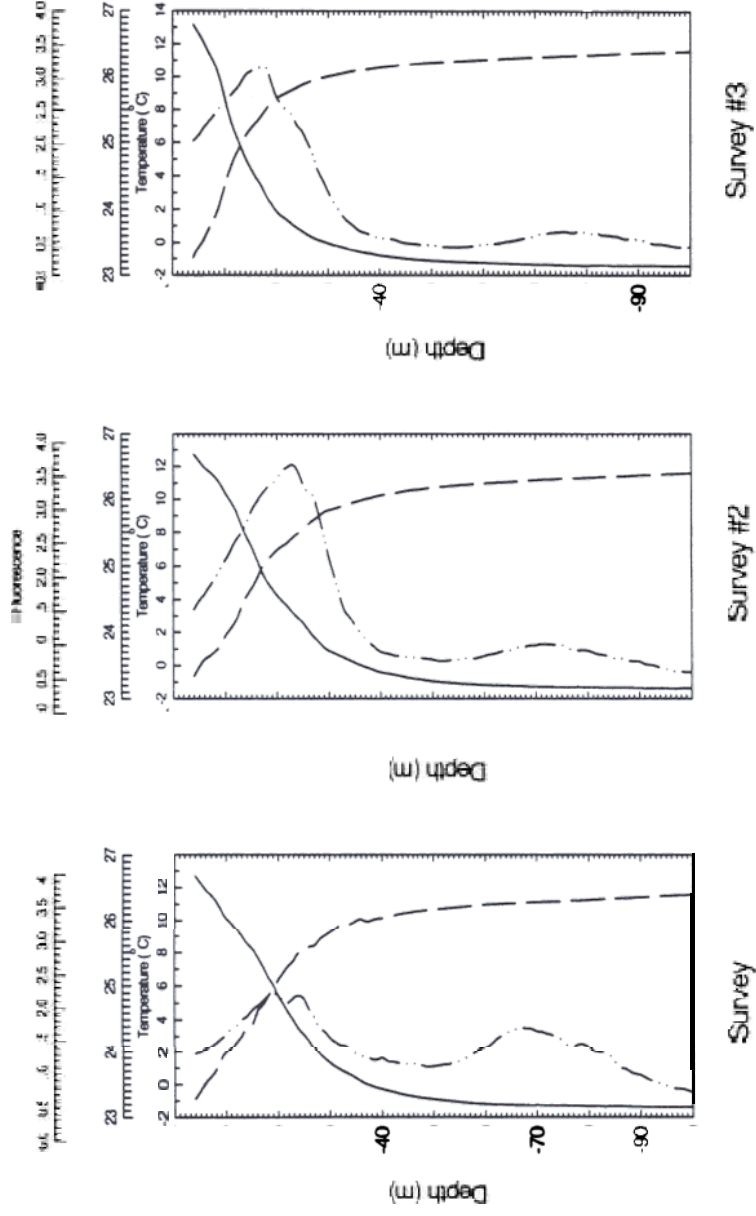


Figure 5 Interpolated view of nauplii concentration ($\# \text{ m}^{-3}$) and **EK500** hydroacoustic integration (Sv) from the three successive surveys. The **scalebar** for each column is located next to the centre panel.

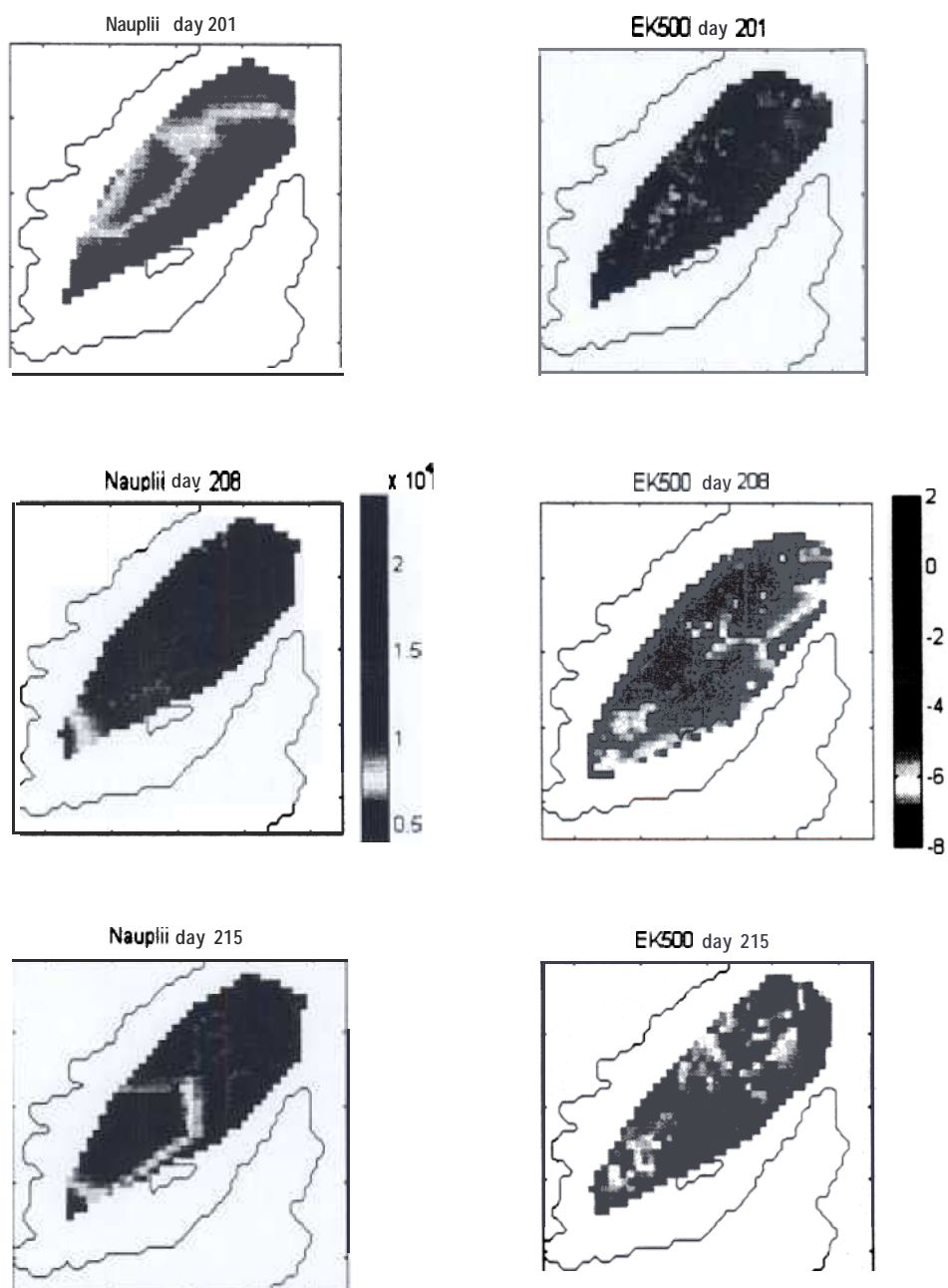


Figure 6. Plot of forward drift projections for particles during the first (day 201-208) and second (day 208-215) week of the study period. For each simulation, the initial position of particles in these plots started from stations 3 (black ●), 5 (blue □), 7 (magenta *); 9 (yellow x); 12 (green +); 14 (cyan 0) and 16 (red ▼) (see Fig.1).

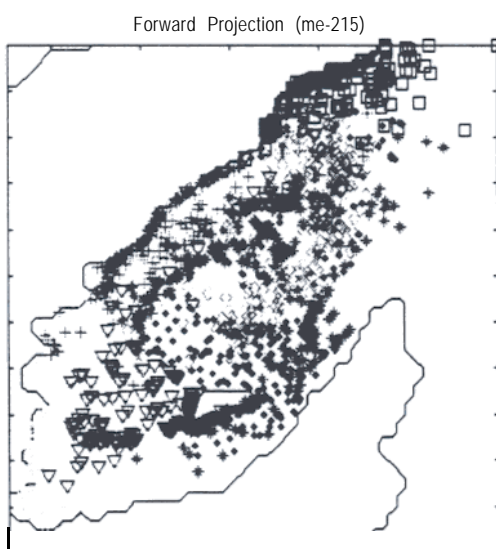
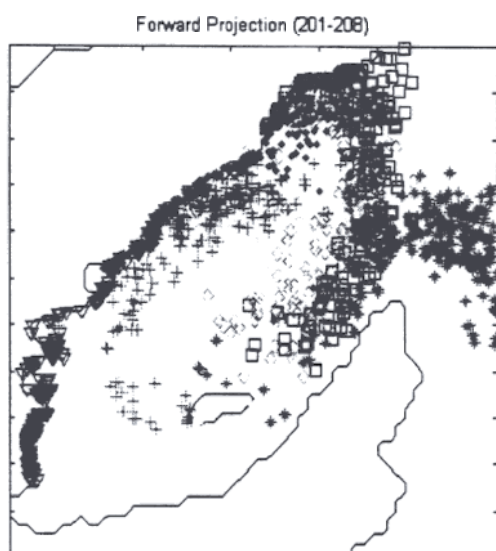


Figure 7. Forward projection of particle locations for stations 1 (red v), 2 (green Cl), 10 (blue •), 11 (magenta x), 12 (yellow 0) and 16 (cyan v) from Fig. 1. These station locations are considered to be in the inner portion of the bay.

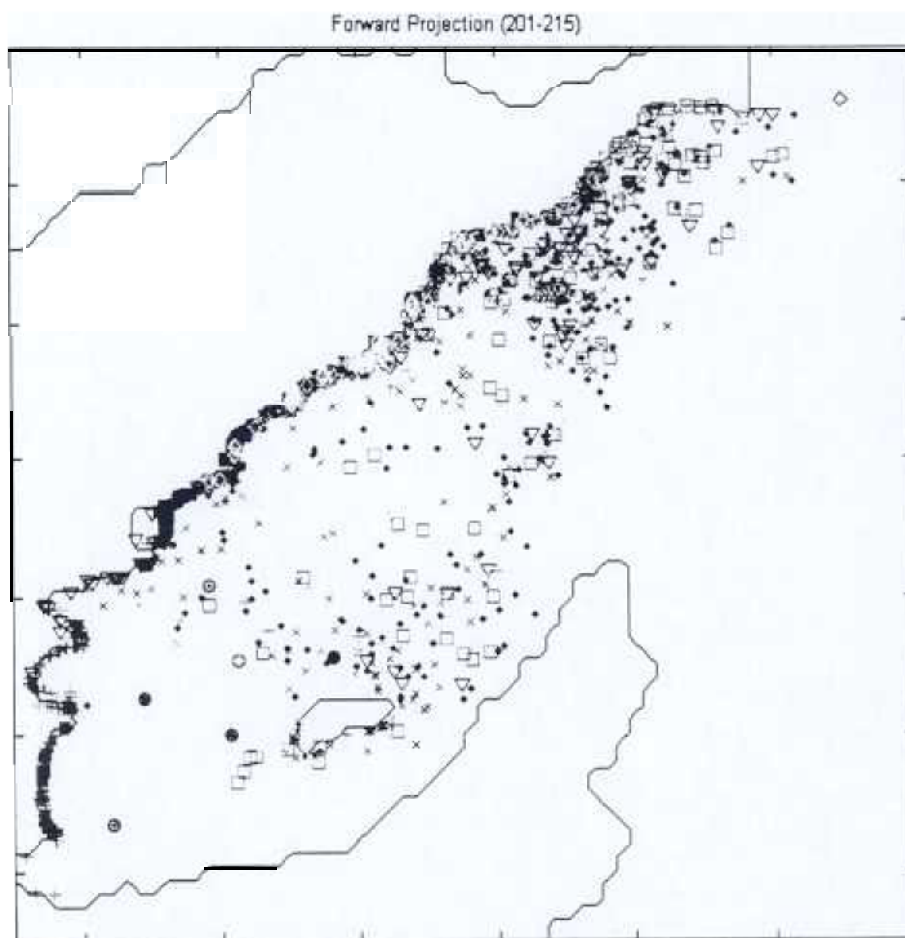


Figure 8 Concentration (# 1000 m⁻²) of radiated shanny larvae from surveys #1 (day 201), #2 (day 208) and #3 (day 215). The length class of larvae is indicated at the top each panel. To follow a cohort between successive surveys, contrast the distribution of larvae of length l with larvae of length $l+2$ in the following survey. Purples indicate areas of high concentrations, reds indicate areas of low concentration.

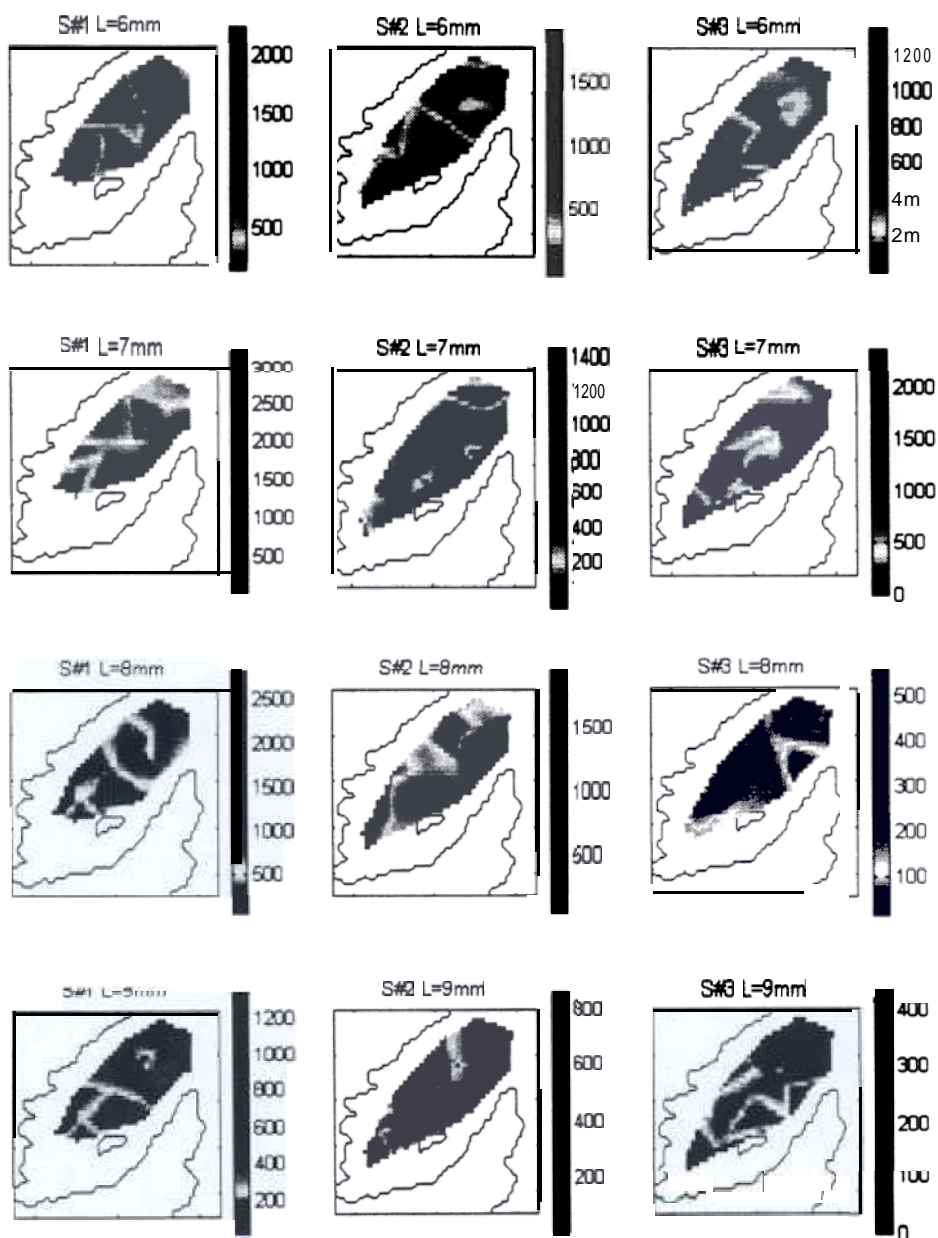


Figure 8. Continued

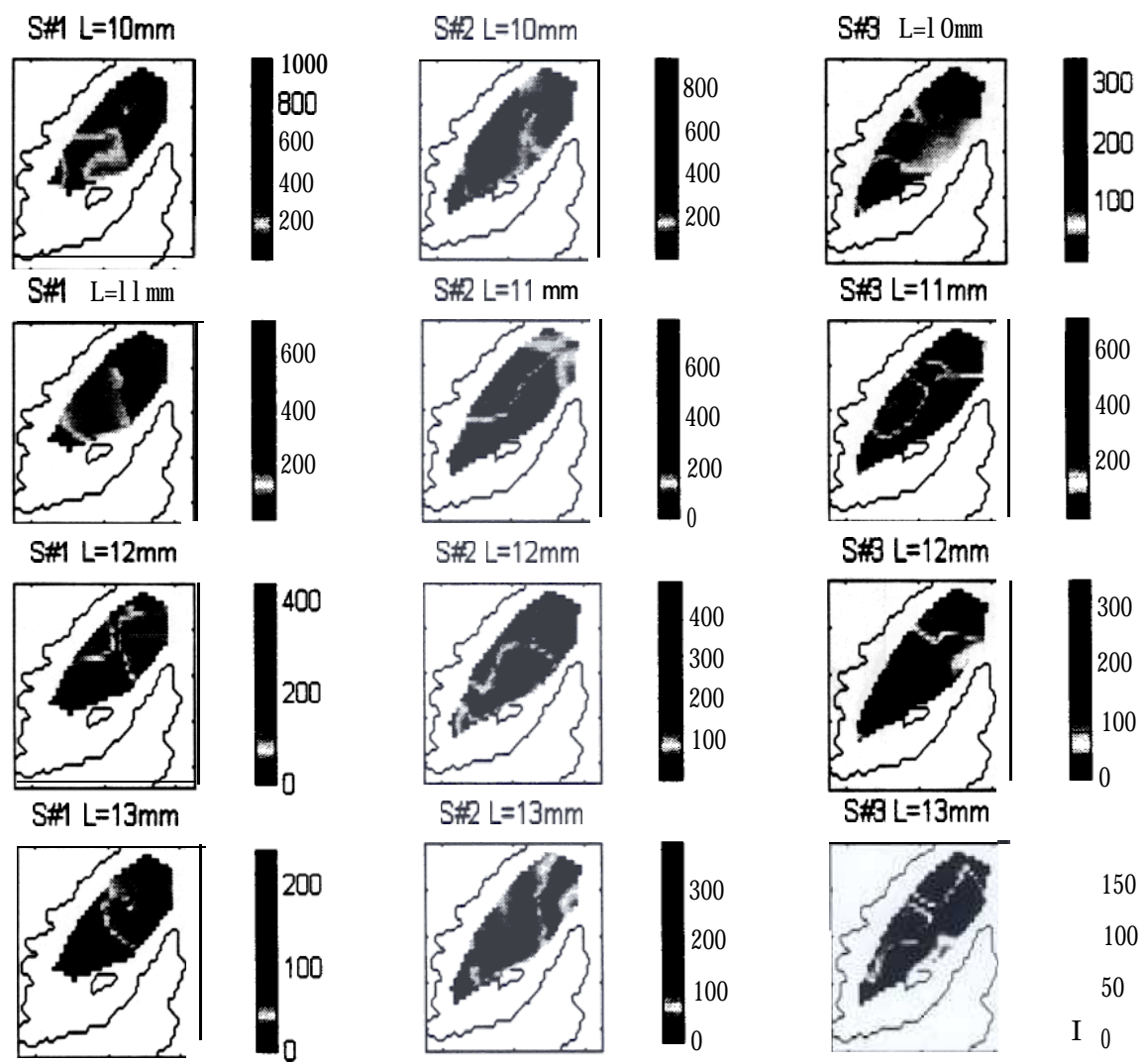


Figure 9. Reconstructed time series of environmental conditions (Nauplii: left column; Predators: right column) in relation to day of year for the first (Top row) and second (Bottom row) weeks of the study period. Drift projections were run for a only one week to limit the effects of dispersal on the reconstructed history of larvae from each station location. Backward projections were run to determine the feeding history of individuals captured from each station and forward projections **were** run to describe the predator environment larvae would face. Each line represents the path of a single station.

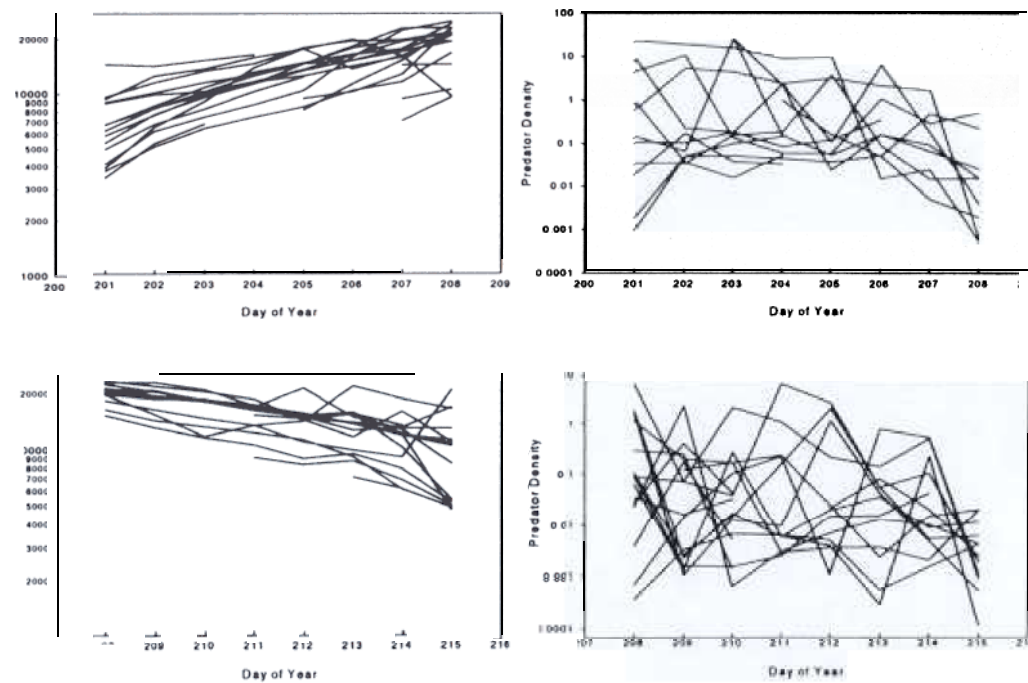


Figure 10. Length at age relationships for radiated shanny larvae captured during each of the three survey periods.

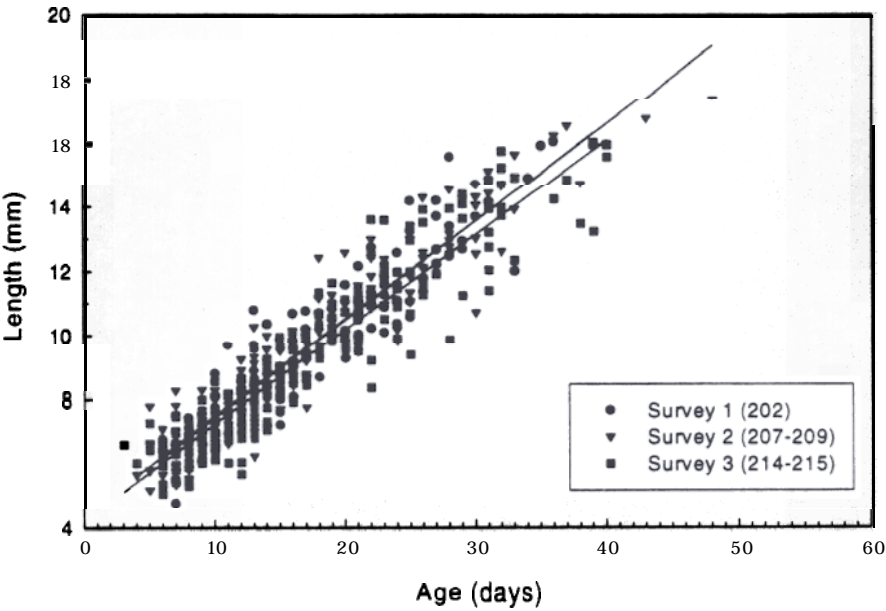


Figure 11. Regression coefficients of the relationship between current growth rates (total age of the larva on the day represented by each increment), the mean increment width at the start of the survey period (based on the three increments prior to days 201 or 208), the concentration of nauplii on the day of the growth increment, and the lag forward from day 201 or 208. Open symbols indicate a non-significant effect whereas closed symbols indicate $p < 0.05$.

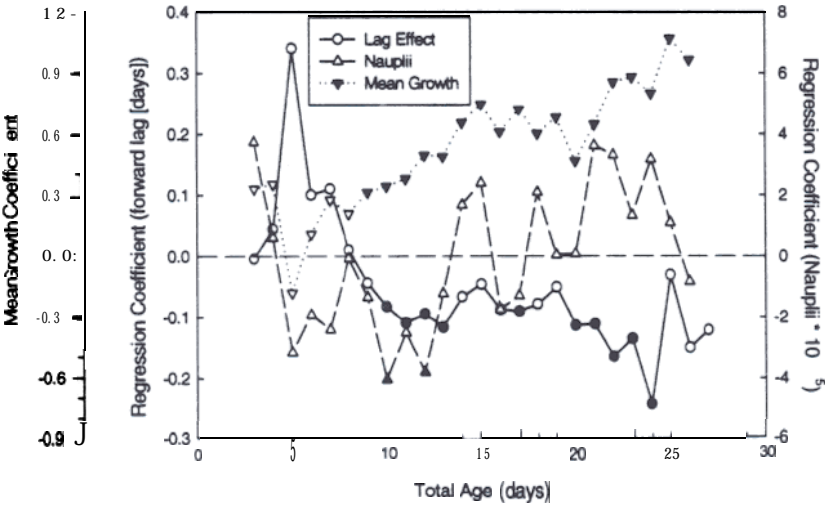


Figure 12. Total mortality during a one week period (Day **201-208**: closed circle; day 208-215: open circle) in relation length of larvae at the start of each survey period (Top panel) and in relation to integrated predator abundance (measured as the summed hydroacoustic integrated voltage for each day) (Bottom panel). In the top panel, symbols for the second week (day 208-215) are slightly offset to show the contrast between weeks.

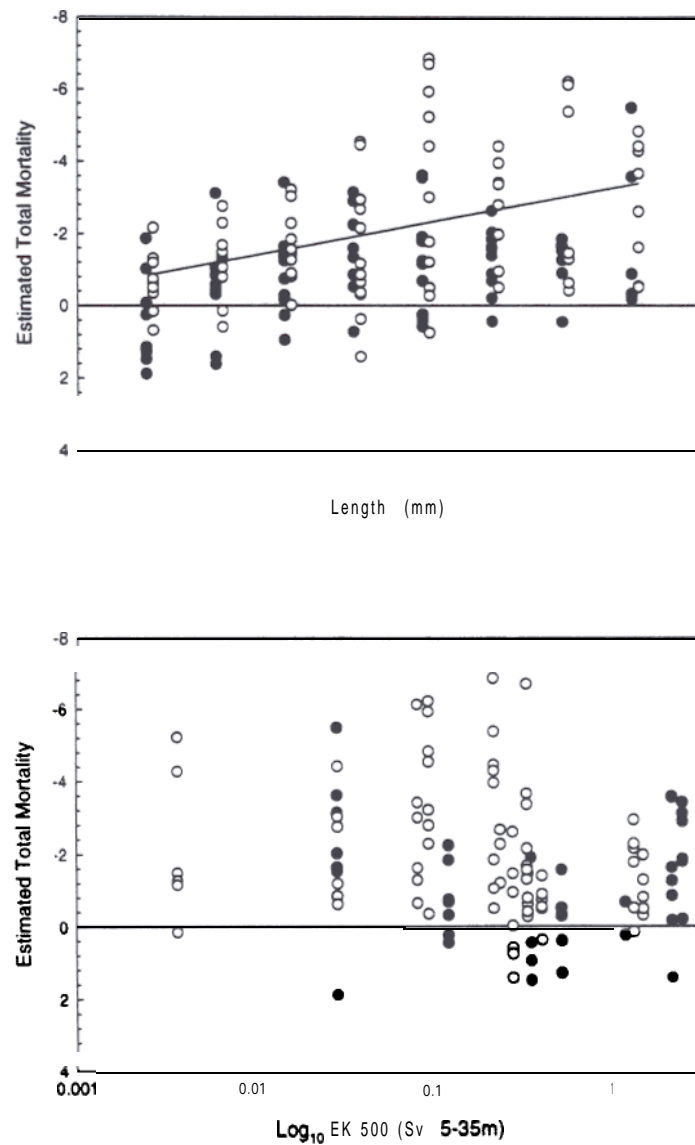


Figure 13. Three dimensional, linearly interpolated surface of the total weekly mortality rate of larval radiated shanny in relation to their length at the start of the week and the summed hydroacoustic integrated voltage. The line and symbol plot on the back panel shows the regression coefficient of the relationship between mortality rate and summed hydroacoustic integrated voltage for each 1 mm length interval.

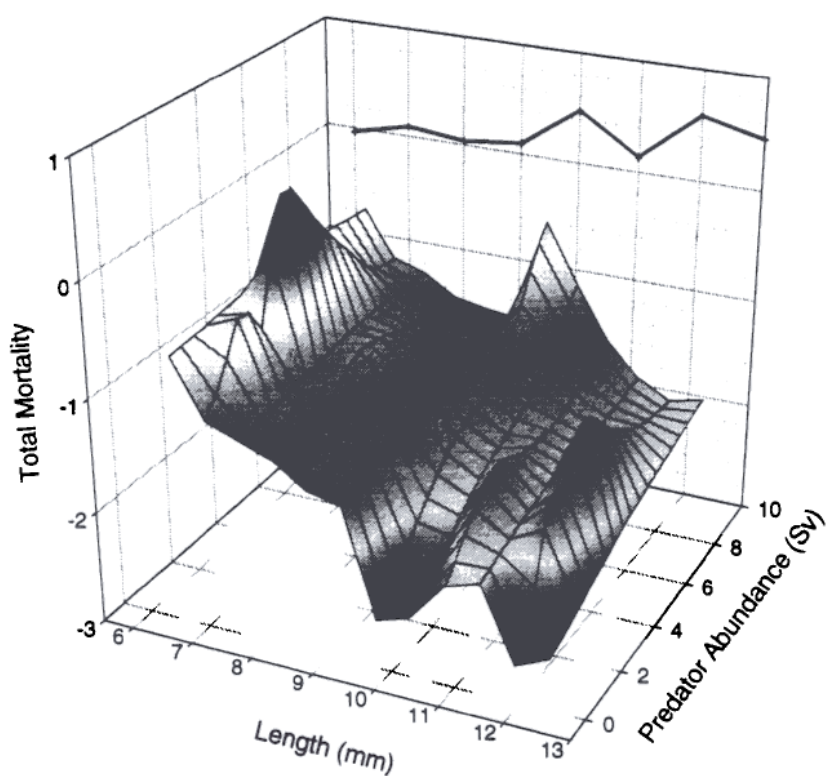


Figure 14. Williamson et al's (1989) index of overlap between larvae and their predators (measured as the hydroacoustic integrated voltage) in relation to larval length during the first (closed symbol) and second (open symbol) surveys.

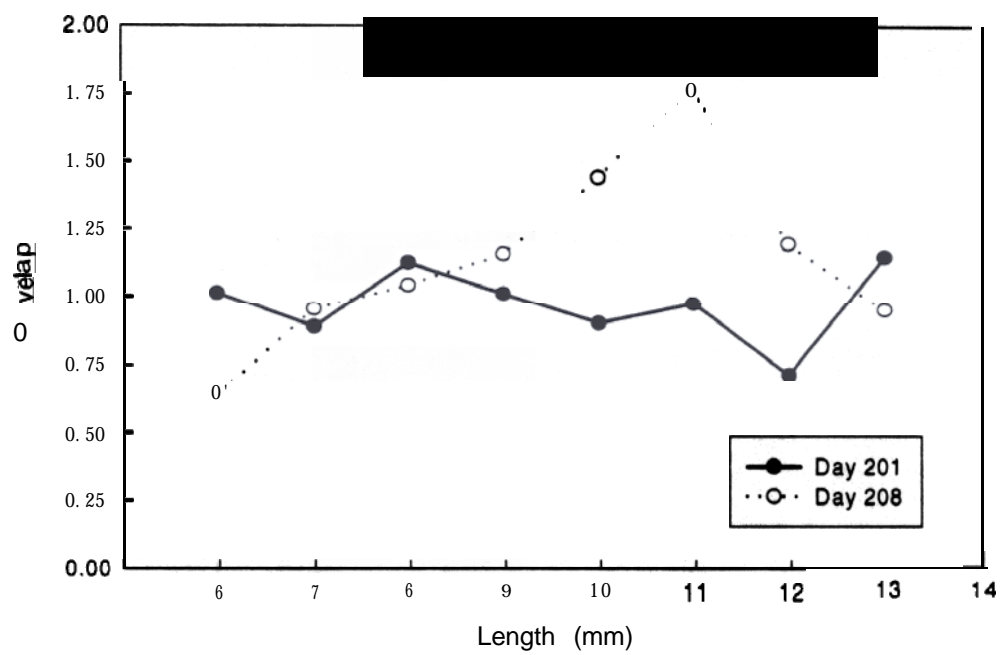


Figure 15. Cumulative probability distribution (**CDF**) of standardized increment widths, based on the three days prior to collection of each specimen, in relation to total age at capture. The three lines show the 10th, 50th and 90th percentiles of the estimated using a local non-parametric density estimator with a bandwidth of 3 days. Inner and outer portions of the bay are identified in Fig. 1.

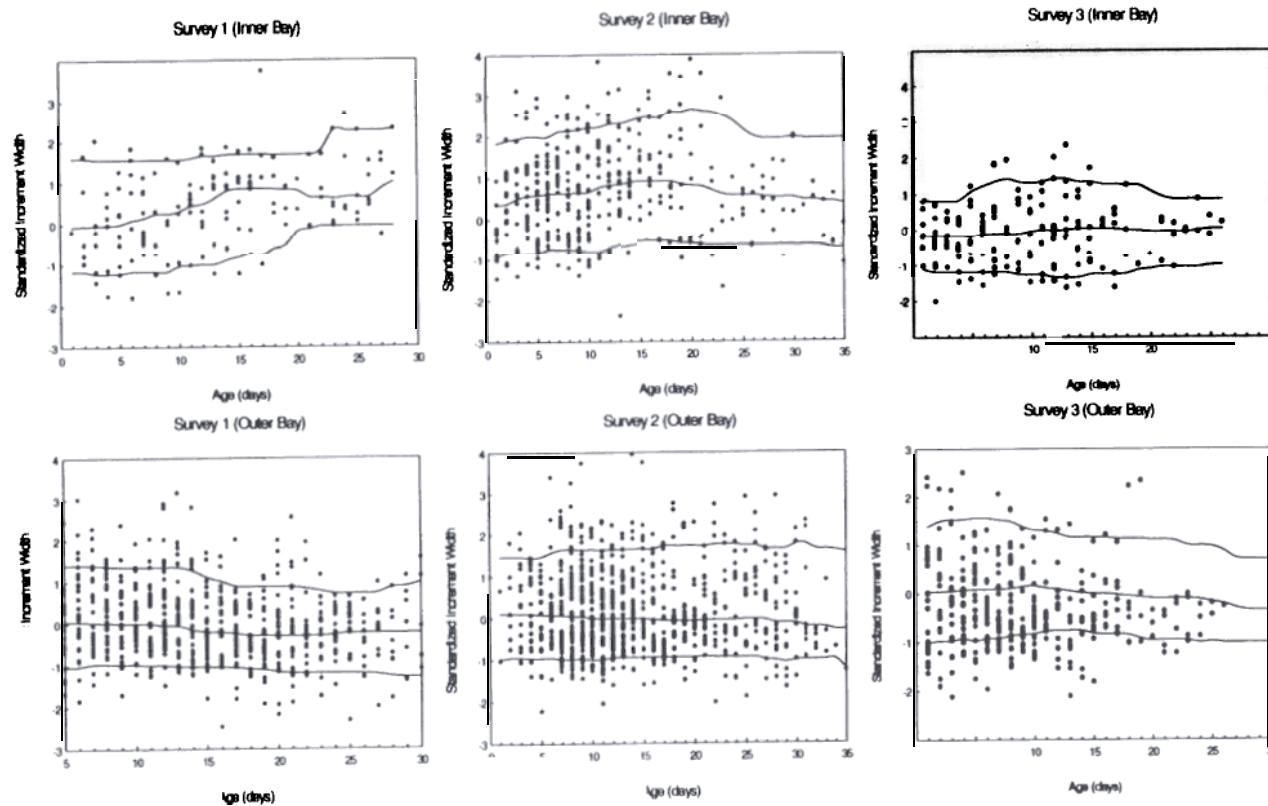


Figure 16. Median and 95% confidence intervals of the median from cumulative probability distribution (CDF) of growth rates in relation to age on day 201 (based on the three standardized increment widths prior to that day) for radiated shanny larvae (Survey #1) from the inner and outer portions of Conception Bay. The larvae used to represent the CDF from each survey are based on the location of capture during each of the surveys. The inner and outer portions of the bay are defined in Fig. 1. The confidence intervals of the median were estimated from 500 randomizations of the data.

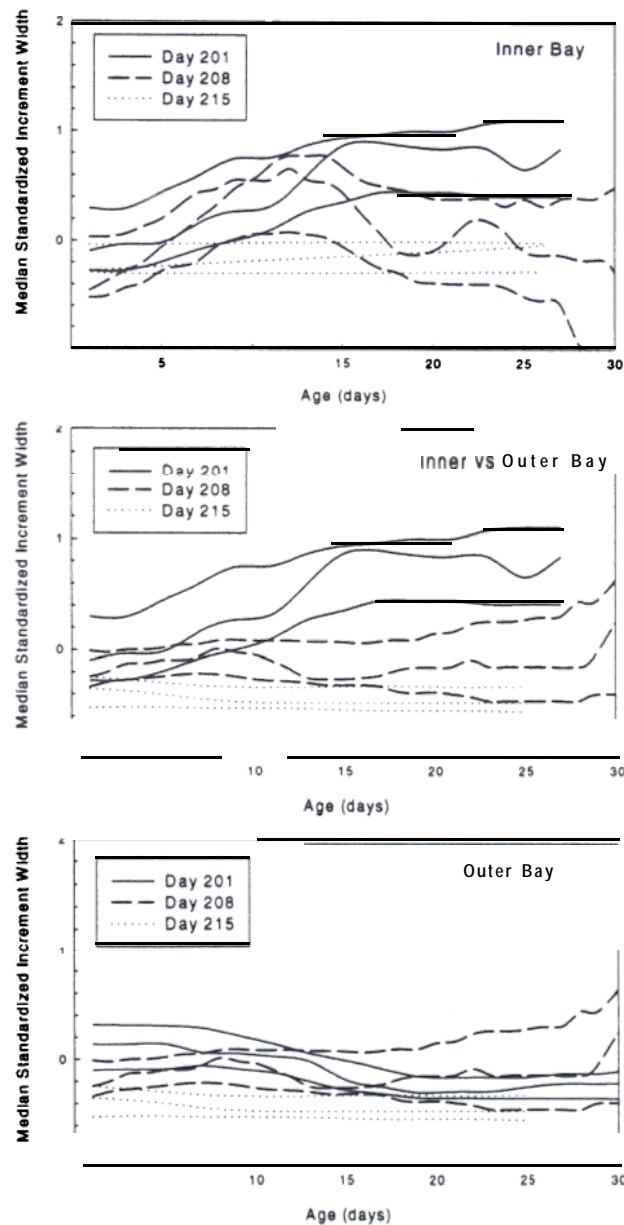


Figure 17. Median and 95% confidence intervals of the median from cumulative probability distribution (**CDF**) of growth rates in relation to age on day 208 (based on the three standardized increment widths prior to that day) for radiated shanny larvae (Survey #2) from the inner and outer portions of Conception Bay. The larvae used to represent the CDF from each survey are based on the location of capture during each of the surveys. The inner and outer portions of the bay are defined in Fig. 1. The confidence intervals of the median were estimated from 500 randomizations of the data.

